Advances in Research

19(4): 1-20, 2019; Article no.AIR.49619
ISSN: 2348-0394, NLM ID: 101666096

Shear Strengthening of R.C Beams with FRP Using (NSM) Technique

Ahmed H. Abdel-Kareem[1], Ahmed S. Debaiky[1], Mohamed H. Makhlouf[1] and M. Abdel-Baset[1*]

[1]Department of Civil Engineering, Benha Faculty of Engineering, Benha University, Egypt.

Authors' contributions

This work was carried out in collaboration among all authors. All authors read and approved the final manuscript.

Article Information

DOI: 10.9734/AIR/2019/v19i430129
Editor(s):
(1) Dr. Carlos Humberto Martins Professor, Department of Civil Engineering, The State University of Sao Paulo, Brazil.
Reviewers:
(1) S. Suppiah, Vel Tech R. Rangarajan, Dr. Sagunthala, R & D Institute of Science and Technology, India.
(2) Md. Akter Hosen, University of Malaya, Malaysia.
Complete Peer review History: http://www.sdiarticle3.com/review-history/49619

Original Research Article

Received 15 April 2019
Accepted 21 June 2019
Published 28 June 2019

ABSTRACT

This paper presents the experimental results of investigations the shear behavior of strengthened reinforced concrete beams by using glass fiber reinforced polymers (GFRP) rods. The strengthening system used GFRP rods were done by Near Surface Mounted technique (NSM), NSM technique contains a groove on the outside surface of the concrete member to adjust the depth to be less than the cover of the member. After cleaning, the epoxy paste was used to fill half of the groove's depth. The particular FRP element is then mounted in the groove. Finally, the groove is filled with epoxy and the too much epoxy is leveled with the outside surface of the concrete. This method enables the fiber reinforcement polymer FRP materials is covered completely by epoxy. The main objective of this research is to study the effect of NSM technique on shear resistance for RC beam. The parameters are considered in this study are effect of the material type used for strengthening (inner steel stirrups and external glass fiber stirrups), effect of FRP rods inclination on strengthened beams, shape with different end anchorage of FRP (strips and rods), and the effect of number of the used FRP rods. This paper involved 13 experimental investigations of half-scale R.C beams. The experimental program included two specimens strengthened with inner steel stirrups, eight specimens strengthened with stirrups of Glass Fiber Reinforced Polymer GFRP rods with the shape of different end anchorage and angle, and two specimens strengthened with externally bonded GFRP strips. The remaining un-strengthened specimen was assigned as a control one for

**Corresponding author: E-mail: mo.baset@yahoo.com;*

comparison. The test results included ultimate capacity load, deflection, cracking, and mode of failure. All beams strengthened with GFRP rods showed an increase in the capacity ranging between 14% to 85% comparing to the reference beam, and beams strengthened with GFRP strips showed an increase in the capacity ranging between 7% to 22% comparing to the reference beam.

Keywords: Fiber Reinforced Polymer (FRP); Reinforced Concrete (R.C); Near Surface Mounted (NSM); strengthening; shear.

1. INTRODUCTION

Many existing reinforced concrete RC elements are exposed to damage due to harsh environmental conditions. These include high temperatures, humidity, and exposure to salt water. These severe environmental conditions result in significant deteriorations of concrete structures mainly due to steel corrosion problems [1]. Shear failure is catastrophic and occurs usually without advance warning. Thus, it is desirable that the beam fails in flexure rather than in shear. Deficiencies for shear occur for several reasons, including insufficient shear reinforcement or reduction in steel area because of corrosion, increased service load, and construction defects. Repairing these elements is costly and demanding a lot of strengthening techniques have been carried out to repair the degraded elements formerly. Traditional methods for enhancement of reinforced concrete RC beams increase the area of the cross-section and adding additional tension steel reinforcement which is a waste of time and expense. At the inception, external post-tensioning and additional externally bonded steel plates using epoxy were used to increase the load carrying capacity of reinforced concrete RC members because of the ease of installation and economic feasibility of these techniques. However, these techniques showed durability limitations because of potential corrosion, heavyweight and practical difficulties with respect to external post-tensioning. Hence, the need for a corrosion free material for retrofitting techniques arose. The advancements in the area of fiber reinforced polymer FRP composites in aerospace applications brought attention to their potential in civil engineering applications. FRP resistant to corrosion and thus help us to improve strength and durability. Generally, the FRP materials consist of fibers that are impregnated in the matrix of vinyl ester which convert the loads between the fibers and protect them. The fibers could be made from glass, aramid, and Carbone.

In order to increase the shear resistance of concrete beams, sheets and laminates of FRP are generally applied on the faces of the elements to be strengthened, using an externally bonded reinforcing (EBR) technique. Several researchers have verified that the shear resistance of concrete beams can significantly be increased by adopting the EBR technique. Over the past two decades, shear and/or flexural strengthening with externally bonded FRP laminates have become a celebrated and promising technique owing to extensive experimental tests [2,3,4,5], analytical investigations [6,7,8] and nonlinear finite element models [9,10] conducted in the field. But this technique cannot mobilize the full tensile strength of FRP materials, due to premature debonding from the concrete substrate. Since FRP systems are directly exposed to weathering conditions, negative influences of freeze/thaw cycles and the effect of high and low temperatures should be taken into account in the reinforcing performance of these materials. In addition, EBR systems are susceptible to fire and act of vandalism.

Near surface mounted (NSM) technique had been also introduced as a more efficient alternative in FRP strengthening of RC beams [11,12,13,14]. In this technique, a pre-cut groove using saw is made on the tension surface/face of the beam. The groove is half filled with construction adhesive, and then the FRP bar is pressed inside the groove such that half of the circumferential perimeter of the bar is covered with adhesive. Thereafter, the groove is completely filled with adhesive. NSM had been suggested as a promising technique for improving the performance of structurally deficient RC structure, because of its ease of installation. However, research showed that the performance of this technique is strongly dependent on the bond performance between epoxy-concrete and epoxy-FRP rod. Various studies on the performance of FRP as shear reinforcement are reported in the literature. As per Khalifa and Nanni [15], the strengthening technique using CFRP sheets can be used to increase the shear capacity significantly. Rizzo and De Lorenzis [16] suggested that the NSM

FRP reinforcement significantly enhanced the shear capacity of RC beams also in the presence of a limited amount of steel shear reinforcement. De Lorenzis and Teng [17] had discussed the issues raised by the use of NSM FRP reinforcement such as optimization of construction details, models for the bond behavior between NSM FRP and concrete, reliable design models for flexural and shear strengthening and the maximization of the advantages of this technique. They also gave a critical review of existing research in this area, identified gaps of knowledge and outlined directions for further research. The study by Jayaprakash et al. [18] confirmed that the bi-directional CFRP strip strengthening technique contributes shear capacity to reinforced concrete rectangular shear beams. The study also showed that the external CFRP strip acts as shear reinforcement similar to the internal steel stirrups. Hassan and Rizkalla [19] investigated the feasibility of using different strengthening techniques as well as different types of FRP for strengthening concrete structures. Test results showed that the efficiency of NSM CFRP strips was three times that of the EBR CFRP strips. Kachlakev and McCurry [20] showed that the addition of GFRP alone for shear was sufficient to offset the lack of steel stirrups and allow conventional RC beam failure by yielding of the tension steel. Sundarraja and Rajamohan [21] have conducted experiments on reinforced concrete beams externally strengthened with GFRP inclined strips as shear reinforcements. The effectiveness of side strips was compared with that of the U-wrap strips. The ultimate loads of beams retrofitted with U-wrapping were greater than the beams retrofitted by bonding the GFRP strips on the sides alone. The test results by Täljsten and Elfgren [22] proved that a very good strengthening effect in shear could be achieved by bonding fabrics to the face of concrete beams. Hassan and Rizkalla [23] showed that the use of NSM CFRP strips substantially increases the stiffness, strength, debonding loads and bond characteristics of concrete beams. Zhang and Hsu [24] concluded that the FRP system can significantly increase the serviceability, ductility, and ultimate shear strength of a concrete beam, thus restoring beam shear strength by using FRP is an effective technique.

2. EXPERIMENTAL PROGRAM

This study involves the implementation of the Near Surface Mounted strengthening technique to increase the shear resistance of concrete beams using GFRP. The NSM technique is based on fixing GFRP into pre-cut slits opened in the concrete cover of lateral surfaces of the beams using adhesive. To assess the efficacy of this technique, an experimental program was carried out on reinforced concrete beams failing in shear. One beam was taken as a reference beam which is not strengthened. The beams strengthened using the NSM method was classified into two series of beam specimens. The first series, series A consists of ten strengthened beam specimens. two specimens strengthened with steel stirrups at spacing 200 mm and 150 mm respectively, two specimens each were strengthened with NSM GFRP rods with U-shape at angle 90° and 45º respectively, two specimens each were strengthened with NSM GFRP rods with Box-shape with cap at angle 90º and 45º respectively, two specimens each were strengthened with NSM GFRP rods with U-shape with anchorage at angle 90º and 45º respectively, two specimens each were strengthened with NSM GFRP rods with U-shape with strand at angle 90º and 45º, respectively. The second series, series B consists of two strengthened beam specimens. Two specimens each were strengthened with EBR GFRP strips with Box-shape and U-shape with the top rod at angle 90º respectively. As shown in Table 1.

2.1 Details of Specimens

The size of the beam selected for the study was 150 x 300 x 1700 mm. The beams were designed as shear deficient beams. Three numbers of 16 mm diameter bars were provided as tension reinforcement and two numbers of 10 mm diameter bars were provided as top reinforcement. Three-legged 6mm diameter bars were provided as holding stirrups at both ends of the beam and middle. As shown in Fig. 1.

2.2 Materials

The specimens used in the test program were cast using normal strength concrete with cube strength of 40 MPa. The strengthening materials used were high-grade steel, GFRP rods, and strips. The mechanical properties of these materials were determined from tests carried out according to the specifications of the manufacturers, (Ezz Steel), (Sika Egypt), as shown in Table 2.

Table 1. The distribution of the reinforced concrete beams of the test program

Group	Specimens code	Specimen case	Material	Shape	Spacing (mm)	Angle
Control	**Control**	**Control**	**------**	**---------**	**------**	**------**
	S8-90	Strengthening Beam with NSM	Steel	8Ø6 two branches	200	90
	GR8-BC-90		GFRP	8 Rod (U - shape with cap)	200	90
	GR8-BC-45		GFRP	8 Rod (U - shape with cap)	200	45
A	GR8-U-90		GFRP	8 Rod (U - shape)	200	90
	GR8-U-45		GFRP	8 Rod (U - shape)	200	45
	GR8-UA-90		GFRP	8 Rod (U - shape with anchorage)	200	90
	GR8-UA-45		GFRP	8 Rod (U - shape with anchorage)	200	45
	S12-90		Steel	12Ø6 two branches	125	90
	GR12-BD-90		GFRP	12 Rod (U - shape with strand)	125	90
	GR12-BD-45		GFRP	12 Rod (U - shape with strand)	125	45
	GS8-B-90	EBR	GFRP	8 Strips (Box - shape)	200	90
B	GS8-UR-90		GFRP	8 Strips (U- shape with top rod)	200	90

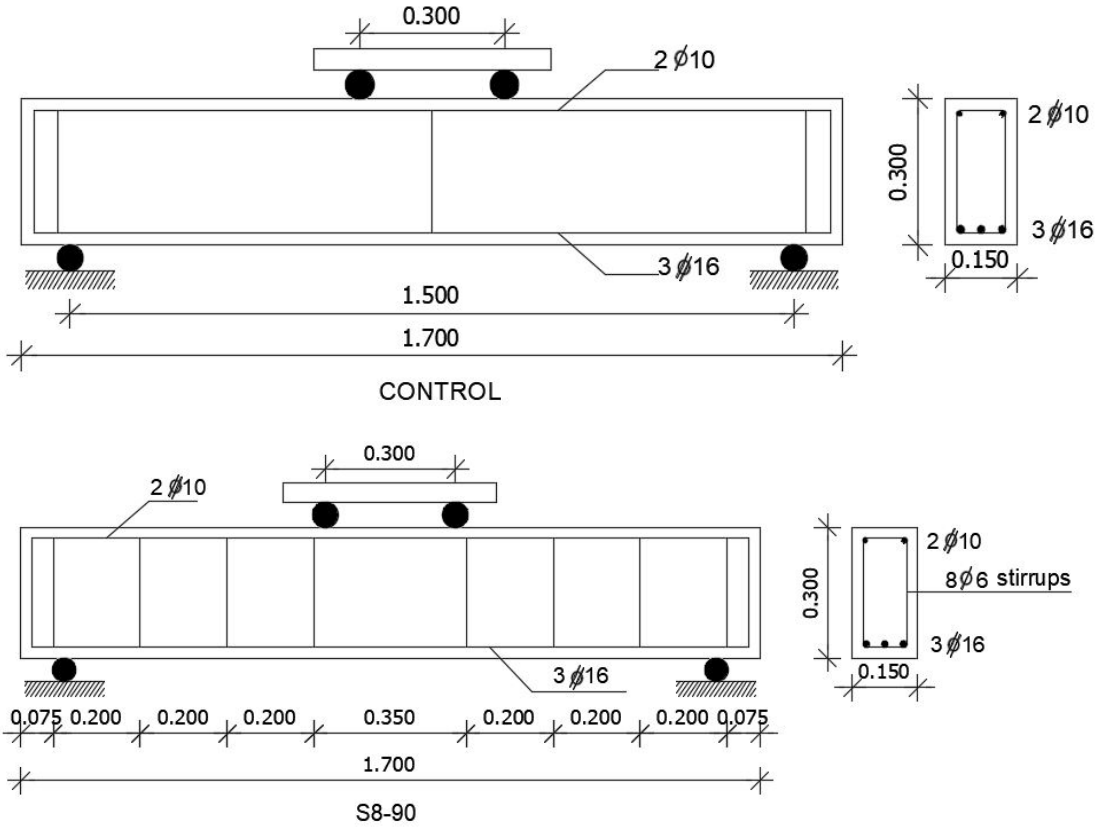

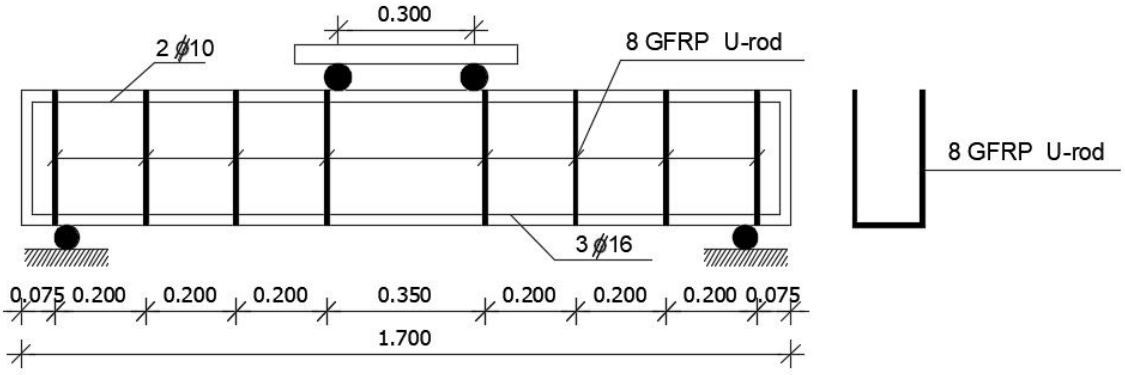

GR8-U-90

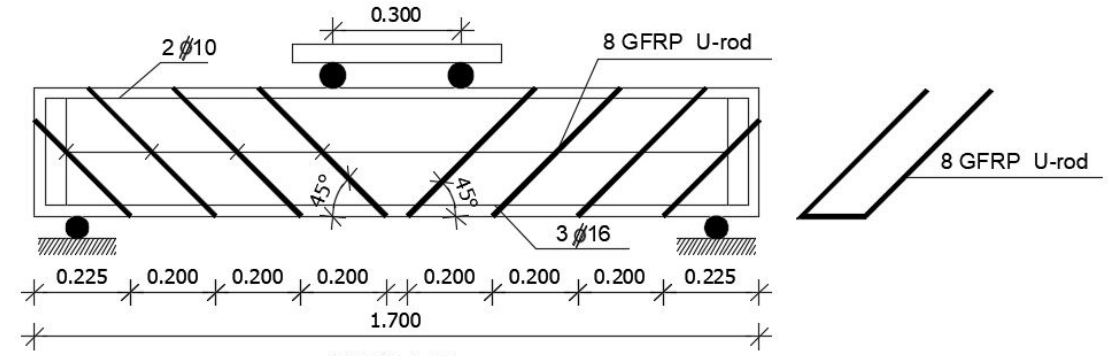

GR8-U-45

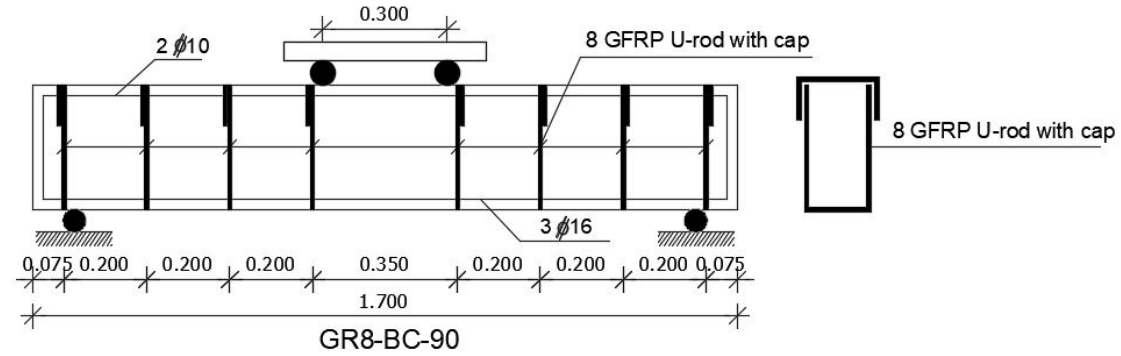

GR8-BC-90

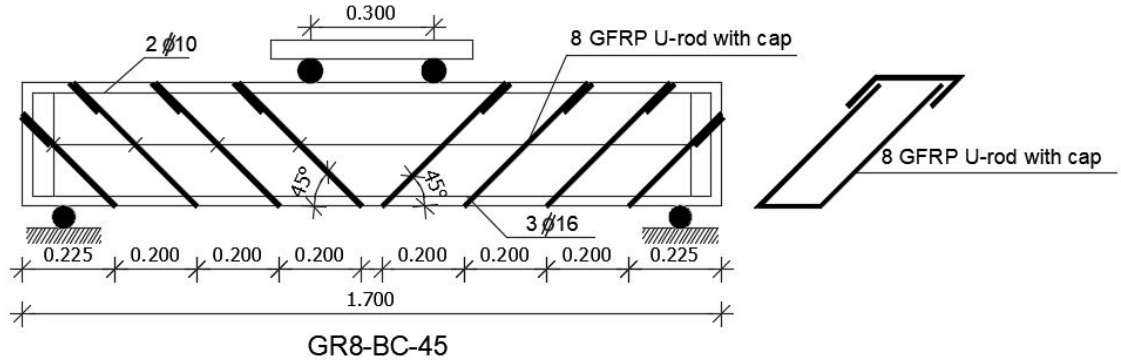

GR8-BC-45

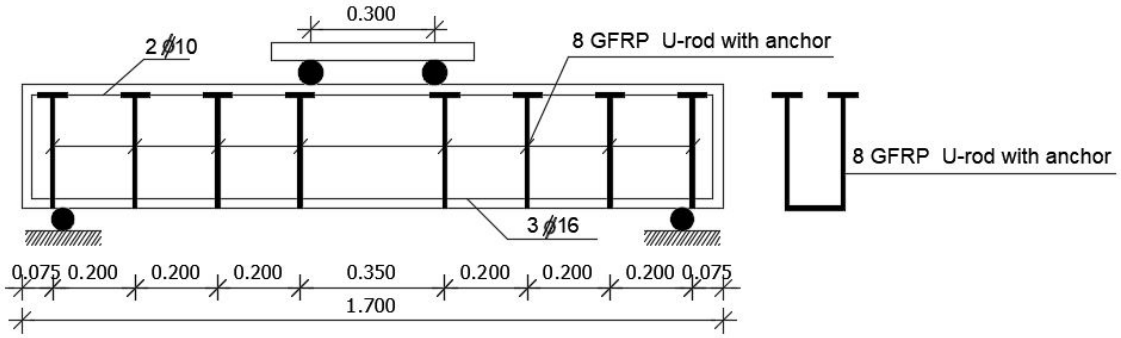

GR8-UA-90

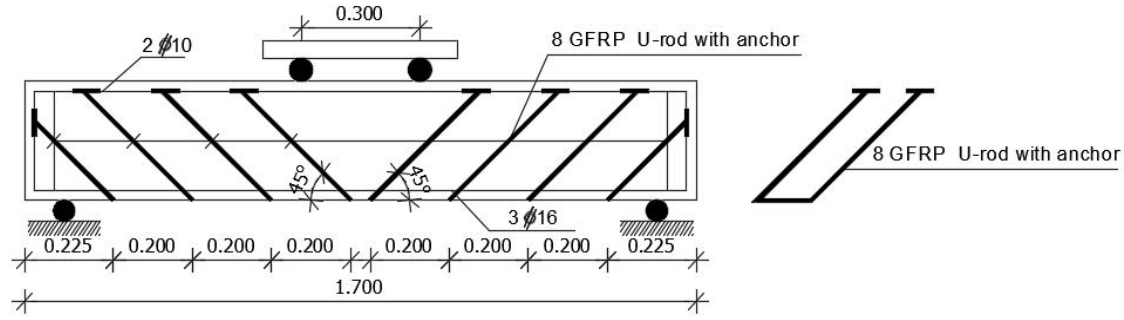

GR8-UA-45

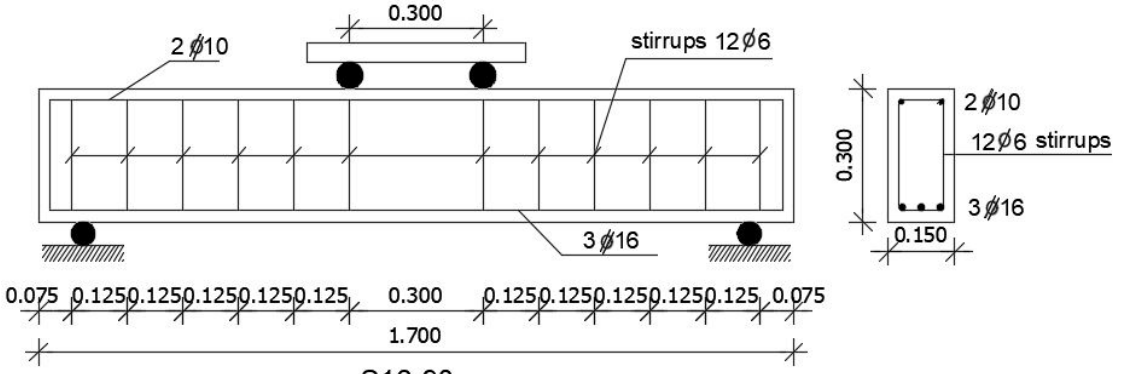

S12-90

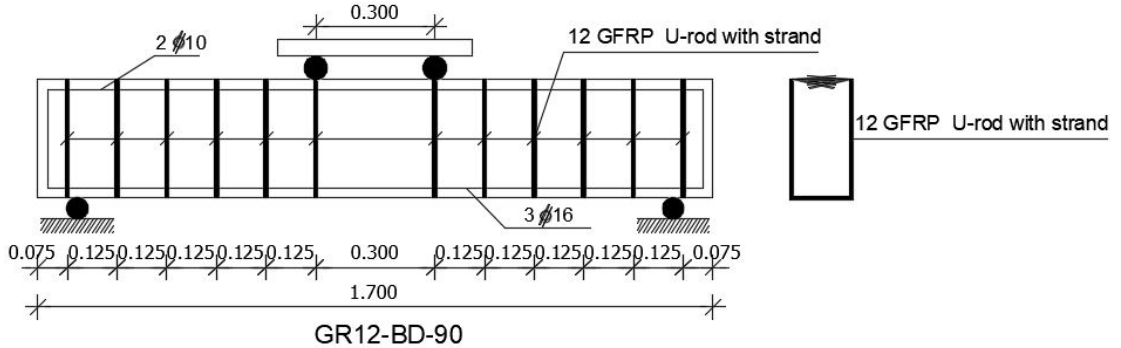

GR12-BD-90

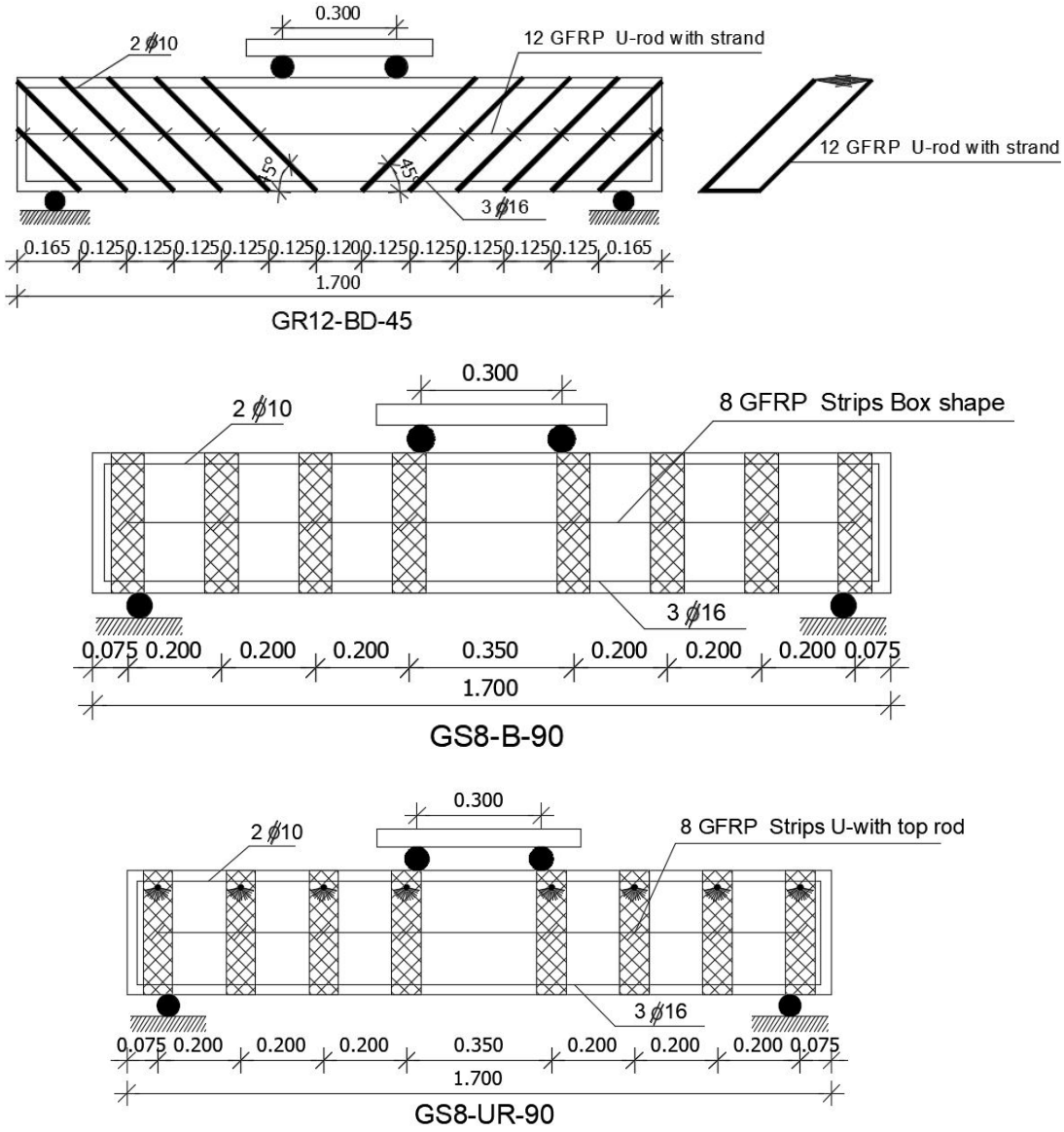

Fig. 1. Dimensions and details of reinforcement of specimens

2.2.1 MMGFRP rods

2.2.1.1 Manufacturing of GFRP rods

The manually made GFRP rod (MMGFRP) was manufactured using FRP strips, where the glass fiber sheet was cut and then wrapped to form a 6 mm diameter rod. Initially, the required width of the FRP sheet (250 mm in this study) was calculated based on the design cross-sectional area. The length of the FRP strip was equal to the length of the MMGFRP rod. A strip with the design width and length was cut from an FRP sheet, then wrapped and placed in the wooden model on which the U-shaped grooved was to be manufactured. The mixed of two-component epoxy resin was then put on the MMGFRP. After that, the trapped air was expelled. After it is finished, it is left to dry and then remove it from the wooden model and manufacture other.

2.2.1.2 MMGFRP anchorage

When the distance between NSM reinforcements in shear enhancement is large, the failure mode is usually NSM debonding, Dias and Barros

(2010). In order to delay the debonding of MMGFRP rods when they are coarsely spaced, an innovative different end anchorage for the MMGFRP rods was proposed in this study. Fig. 2 shows the different shapes of the end anchorage. First, the MMGFRP rod is fabricated with glass fiber sheets and leave part of strip fiber at the end sides dry. Next, The MMGFRP is placed in the grooves on both sides of the beam; the dry fibers at the ends are impregnated with epoxy resin and placed in the grooves. The grooves at end anchorage are perpendicular to the MMGFRP rod when the MMGFRP rods are vertically installed. If the MMGFRP rods are installed not perpendicular to the beam axis, end anchorage is still manufactured to be parallel to the beam axis so in this case, the grooves at end anchorage is not perpendicular to the MMGFRP rod Fig. 3. The main advantage of the proposed anchor system is that it only requires access to the surface of the beams for installation, so that it can be properly applied to RC beams whose top face is inaccessible, such as T-beams. With this anchoring, MMGFRP debonding may be delayed or prevented and more concrete is mobilized to contribute to the shear capacity of the beam.

Table 2. Characteristic properties of steel bars, GFRP rods and GFRP sheets

a) Characteristic properties of steel bars:

Nominal diameter (mm)	Actual area (mm2)	Yield strength (N/mm2)	Ultimate strength (N/mm2)
Φ6	28.3	540	694
Φ10	78.5	490	795
Φ16	201	378	696

b) Characteristic properties of GFRP rods

Characteristic	GFRP rods
Diameter of bars (mm)	6
Area of fibers (mm2)	6.06
Tensile strength (N/mm2)	1375
Modulus elasticity (N/mm2)	66245

c) Characteristic properties of GFRP sheets

Characteristic	GFRP Sheets
Fabric width (mm)	600
Fabric thickness (mm)	0.17
Tensile strength (N/mm2)	2300
Modulus elasticity (N/mm2)	76000

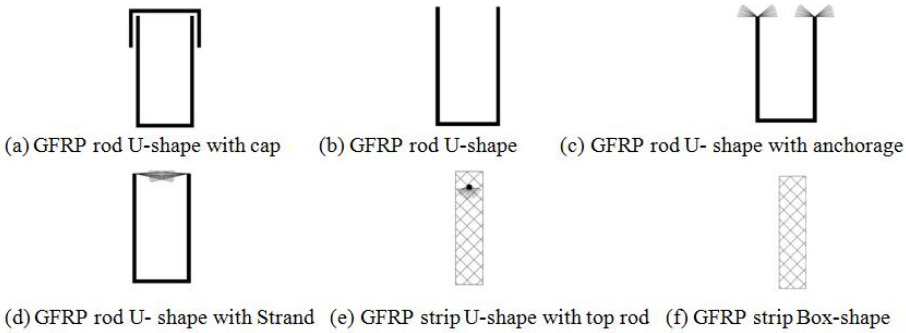

Fig. 2. Different shapes of the end anchorage

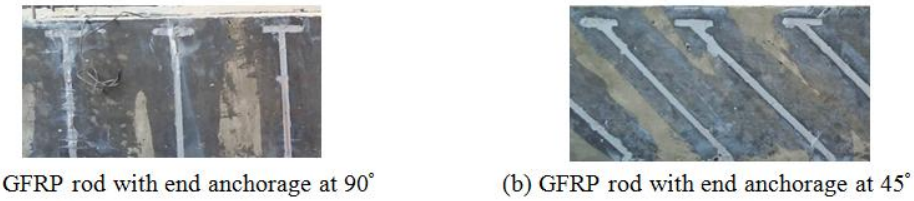

Fig. 3. The end anchorage

2.3 Strengthening of Specimens

In order to strengthen the shear deficient beams using the NSM technique and EBR technique for comparison, GFRP rods and GFRP strips were provided at various alignments. The Glass Fiber rods had tensile strength 2500 N/mm^2. The GFRP rod with different shape was provided at an angle 90º and 45º with the beam axis at the lateral faces for the shear strengthening of the beams. In order to apply the NSM technique, the precast grooves on the lateral surface of the beams were made rough; all grooves had a square cross-section with a nominal depth and width of 10x10 mm, and then cleaned properly using a wire brush. Then the grooves were filled halfway with the groove filler. The surface of the GFRP rods was roughened for ensuring a proper bond between GFRP and the groove filler. Then GFRP is inserted into the groove so the groove filler flows around the GFRP. Then the surface is leveled and smoothened. Then the strengthened beams were left to cure in the air for seven days before testing. As shown in Fig. 4.

In order to strengthen the shear deficient beams using the EBR technique, U wrap of GFRP strips of size 750 mm x 25 mm x 0.17 mm were provided over the entire shear zones. The GFRP used for the EBR application of tensile strength 2300 N/mm^2.

Fig. 4. Cutting groove and placing MMGFRP rods

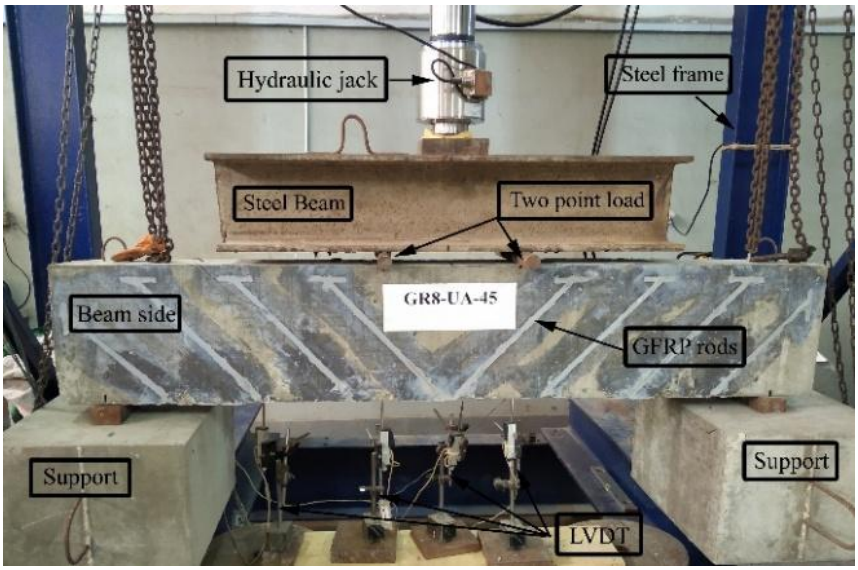

Fig. 5. Beam under test showing LVDT and hydraulic jack

2.4 Testing of Specimens

For the test set-up used in this study consisted of rigid steel frames supported by the laboratory rigid floor. The load was applied using a hydraulic jack of 1000 KN capacity, Load was measured using a load cell connected to the data acquisition system. The beam specimens were tested under two-point loading, as shown in Fig. 5. Four linear variable differential transducers (LVDT) mounted at the bottom soffit of the specimen for measuring deflections, placed at mid-span of the specimen and under two load application points and mid-span of shear. Propagation of cracks was marked gradually up to failure.

3. RESULTS AND DISCUSSION

In this part, the observations during testing and the analysis of the results are briefly described.

3.1 Load – Carrying Capacity of the Tested Specimens

The first crack load and ultimate load for the test specimens are shown in Table 3. The crack pattern of all tested beams is shown in Fig. 6.

3.1.1 Control specimens

Flexural cracking in the reference beam started at the mid-span at a load of P = 75 KN. The first shear crack appeared in about the middle of the test shear span at 82 KN. More flexural–shear cracks formed thereafter within the test shear span. At about 93 KN, these cracks had widened and propagated to form the final crack pattern. The beam failed in shear at P_{max}= 95.9 KN. As shown in Table 3.

3.1.2 Series A

3.1.2.1 Specimen S8-90

For these beam strengthened with steel stirrups, the primary patterns of cracking were similar to that of the (Control) beam, as shown in Fig. 6. The relationship between the maximum load and the deflection at beam mid-span is depicted in Fig. 8(a). Table 3 includes the main results obtained in this specimen. When compared to the maximum load of the (Control) beam, Table 3 shows that the shear strengthening systems with steel stirrups increased the maximum load of 67 %(S8-90). The crack load of this beam S8-90 was 2 % larger than the crack load of the control beam. The deformation capacity was registered in the beam strengthened with steel stirrups corresponding to the max load. In comparison with Δ_{ul-c} (control beam), the Δ_{ul-s} is 93 % larger. The deformation capacity corresponding to the crack load Δ_{cr-s} in this beam S8-90 was 12 % larger than the deformation capacity corresponding to the crack load in the (Control) beam Δ_{cr-c}.

3.1.2.2 Specimens GR8-U-90 and GR8-U-45

For these beams strengthened with GFRP by (NSM) technique with rods (U-shape), Fig. 6 shown the crack pattern in these specimens. The relationship between the maximum load and the deflection at beam mid-span is depicted in Fig. 8(a). Table 3 includes the main results obtained in these specimens, taking the maximum load of (Control) beam as a reference value, the GR8-U-90, GR8-U-45 beams provided a 14% and 17% increase in maximum load, respectively, as shown in Fig. 10. The crack load of these specimens GR8-U-90, GR8-U-45 was 4% and 24% larger than the crack load of the (Control) beam, respectively. When compared the maximum load in these specimens with beam strengthening with steel stirrups S8-90 was 32% and 30% less than the maximum load in beam S8-90. The deformation capacity was registered in the GR8-U-90, GR8-U-45 beams, corresponding to the maximum load at beam mid-span. In comparison with Δ_{ul-c} (Control) beam, the Δ_{ul} was 55% and 45% larger, respectively, as showing in Fig. 15. In comparison with Δ_{ul-s} (S8-90 beam), the Δ_{ul} was 19% and 25% less than the deformation capacity corresponding to the maximum load in the S8-90 beam, respectively. The deformation capacity corresponding to the crack load Δ_{cr} in these beams GR8-U-90, GR8-U-45 was 49% and 29% larger than the deformation capacity corresponding to the crack load in the (Control) beam Δ_{cr-c}. Finally, the specimens GR8-U-90, GR8-U-45 failed in shear at maximum load 109.5, 112 KN, respectively.

3.1.2.3 Specimens GR8-BC-90 and GR8-BC-45

For these beams strengthened with GFRP by (NSM) technique with rods (Box – shape with cap), Fig. 6 shown the crack pattern in these specimens. The relationship between the maximum load and the deflection at beam mid-span is depicted in Fig. 8(b). Table 3 includes the main results obtained in these specimens. Taking

the maximum load of (Control) beam as a reference value, the GR8-BC-90 and GR8-BC-45 beams provided a 22% and 26% increase in maximum load, respectively as shown in Fig. 10. The crack load of these specimens GR8-BC-90, GR8-BC-45 was 7% and 32% larger than the crack load of the (Control) beam, respectively. When compared the maximum load in these specimens with beam strengthening with steel stirrups S8-90 was 27% and 25% less than the maximum load in beam S8-90. The deformation capacity was registered in the GR8-BC-90, GR8-BC-45 beams, corresponding to the maximum load at beam mid-span. In comparison with Δ_{ul-c} (Control) beam, the Δ_{ul} was 43% and 13% larger, respectively, as shown in Fig. 15. In comparison with Δ_{ul-s} (S8-90) beam, the Δ_{ul} was 26 % and 41% less than the deformation capacity corresponding to the maximum load in the S8-90 beam, respectively. The deformation capacity corresponding to the crack load Δ_{cr} in these beams GR8-BC-90 and GR8-BC-45 was 69% and 21% larger than the deformation capacity corresponding to the crack load in the (Control) beam Δ_{cr-c}. Finally, the specimens GR8-BC-90, GR8-BC-45 failed in shear at maximum load 117.3, 120.7 KN, respectively. In spite of the used of the cap with GFRP rods in these specimens, there was no significant improvement in the loading capacity in comparison to specimen GR8-U-90, GR8-U-45. See Table 3.

3.1.2.4 Specimens GR8-UA-90 and GR8-UA-45

For these beams strengthened with GFRP by (NSM) technique with rods (U – shape with anchorage), Fig. 6 shown the crack pattern in these specimens. The relationship between the maximum load and the deflection at beam

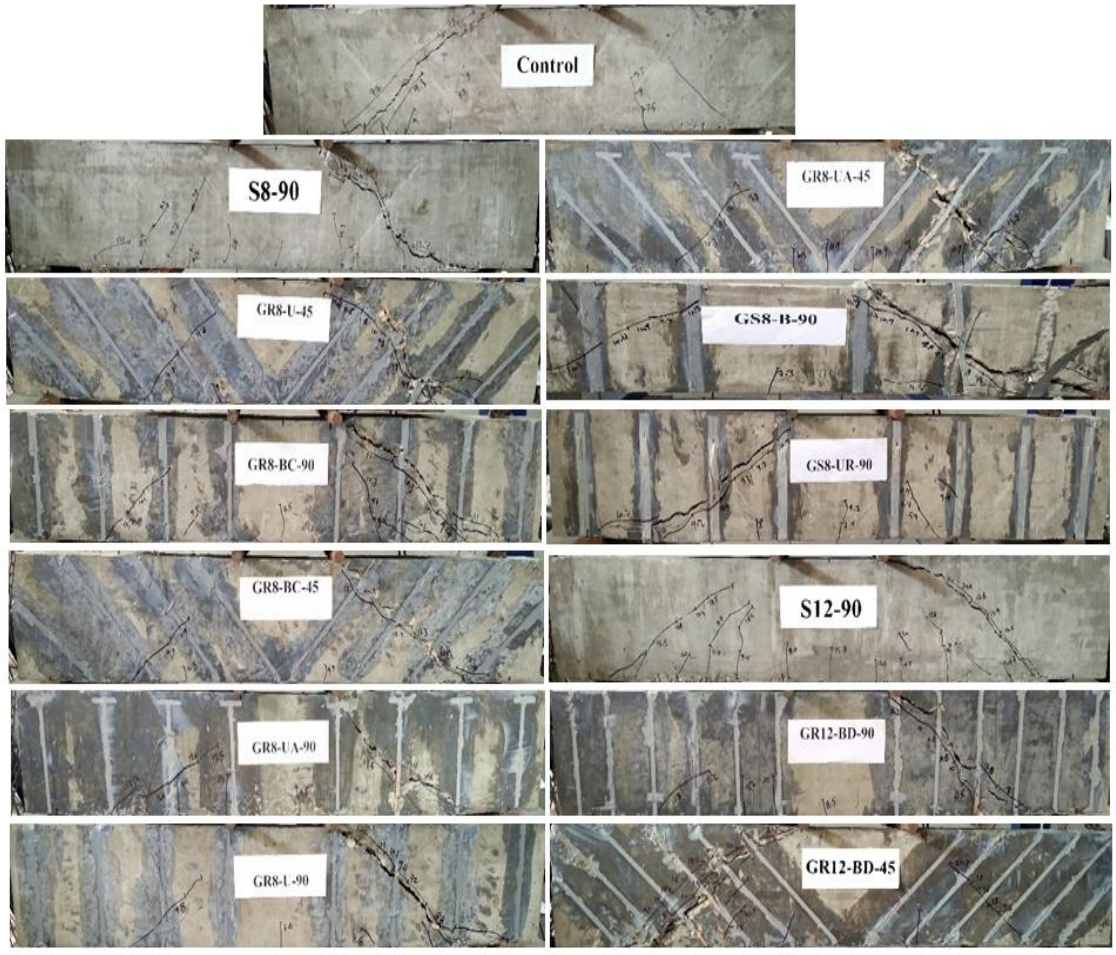

Fig. 6. Crack pattern in test of all beams

Table 3. Experimental results of specimens

Specimen code	P_{cr} (KN)	Δ_{cr} (mm)	P_{ul} (KN)	Δ_{ul} (mm)	Increase over reference beam without any shear reinforcement %				Increase over reference beam with inner steel stirrups %	
					(P_{ul}/P_{ul-c})%	$(\Delta_{ul}/\Delta_{ul-c})$%	(P_{cr}/P_{cr-c})%	$(\Delta_{cr}/\Delta_{cr-c})$%	(P_{ul}/P_{ul-s})%	$(\Delta_{ul}/\Delta_{ul-s})$%
Control	75.00	2.33	95.90	3.59	1.00	1.00	1.00	1.00	0.60	0.52
S8-90	76.50	2.60	160.40	6.93	1.67	1.93	1.02	1.12	1.00	1.00
GR8-U-90	78.00	3.47	109.50	5.58	1.14	1.55	1.04	1.49	0.68	0.81
GR8-U-45	93.00	3.00	112.00	5.22	1.17	1.45	1.24	1.29	0.70	0.75
GR8-BC-90	80.00	3.93	117.30	5.13	1.22	1.43	1.07	1.69	0.73	0.74
GR8-BC-45	99.00	2.82	120.70	4.06	1.26	1.13	1.32	1.21	0.75	0.59
GR8-UA-90	106.00	6.87	150.30	9.49	1.57	2.64	1.41	2.95	0.94	1.37
GR8-UA-45	112.00	4.74	169.03	8.13	1.76	2.26	1.49	2.03	1.05	1.17
S12-90	86.00	1.74	203.20	7.29	2.12	2.03	1.15	0.75	1.00	1.00
GR12-BD-90	81.00	3.28	152.90	6.98	1.59	1.94	1.08	1.41	0.75	0.96
GR12-BD-45	84.50	2.39	177.80	6.73	1.85	1.87	1.13	1.03	0.88	0.92
GS8-B-90	76.50	2.89	116.65	5.72	1.22	1.59	1.02	1.24	0.73	0.83
GS8-UR-90	76.00	2.67	102.40	4.26	1.07	1.19	1.01	1.15	0.64	0.61

Note: P_{cr} : Cracking load; Δ_{cr} : Deflection correspond to P_{cr} ; P_{ul} : Ultimate load; Δ_{ul} : Deflection correspond to P_{ul}

Fig. 7. Close-up view of the failure modes

mid-span is depicted in Fig. 8(c). Table 3 includes the main results obtained in these specimens. Taking the maximum load of (Control) beam as a reference value, the GR8-UA-90, GR8-UA-45 beams provided a 57% and 76% increase in maximum load, respectively, as shown in Fig. 10 where the highest value was registered in the beam strengthened with inclined rods with anchorage GR8-UA-45. The crack load of these specimens was 41% and 49% larger than the crack load of the (Control) beam, respectively. When compared the maximum load in these specimens with beam strengthening with steel stirrups S8-90, the beam GR8-UA-90 was 6% less than the maximum load in beam S8-90, while the beam GR8-UA-45 was the only one that achieved an increase of 5%. The deformation capacity was registered in the GR8-UA-90, GR8-UA-45 beams, corresponding to the maximum load at beam mid-span. In comparison with $\Delta_{ul\text{-}c}$ (Control) beam, the Δ_{ul} was 164% and 126% larger, respectively, as shown in Fig. 15. In comparison with $\Delta_{ul\text{-}s}$ (S8-90) beam, the Δ_{ul} was 37% and 17% larger than the deformation capacity corresponding to the maximum load in the S8-90 beam, respectively. The deformation capacity corresponding to the crack load Δ_{cr} in these beams GR8-U-90, GR8-U-45 was 195% and 103% larger than the deformation capacity corresponding to the crack load in the (Control) beam $\Delta_{cr\text{-}c}$. Finally, the specimens GR8-UA-90, GR8-UA-45 failed in shear at maximum load 150.3, 169.03 KN, respectively, registered with the highest load capacity, especially specimen GR8-UA-45. Clearly the use of GFRP rods with anchored in GR8-UA-90, GR8-UA-45 beams led to a strengthening in both the ultimate strength and the corresponding deflection as shown in Table 3.

3.1.2.5 Specimen S12-90

For these beam strengthened with steel stirrups, Fig. 6 shown the crack pattern in this specimen. The relationship between the maximum load and the deflection at beam mid-span is depicted in Fig. 8(d). Table 3 includes the main results obtained in this specimen. When compared to the maximum load of the (Control) beam, Table 3 shows that the shear strengthening systems with steel stirrups increased the maximum load of 112% (S12-90). The crack load of this beam S12-90 was 15% larger than the crack load of the (Control) beam. The deformation capacity

was registered in the beam strengthened with steel stirrups corresponding to the maximum load. In comparison with Δ_{ul-c} (Control) beam, the Δ_{ul-s} is 103% larger. The deformation capacity corresponding to the crack load Δ_{cr-s} in this beam S12-90 was 25 % less than the deformation capacity corresponding to the crack load in the (Control) beam Δ_{cr-c}.

3.1.2.6 Specimens GR12-BD-90 and GR12-BD-45.

For these beams strengthened with GFRP by (NSM) technique with rods (Box – shape with strand), Fig. 6 shown the crack pattern in these specimens. The relationship between the maximum load and the deflection at beam mid-span is depicted in Fig. 8(d). Table 3 includes the main results obtained in these specimens. Taking the maximum load of (Control) beam as a reference value, the GR12-BD-90, GR12-BD-45 beams provided 59% and 85% increase in maximum load, respectively, as shown in Fig. 10. The crack load of these specimens GR12-BD-90, GR12-BD-45 was 8% and 13% larger than the crack load of the (Control) beam, respectively. When compared the maximum load in this specimens with beam strengthening with steel stirrups S12-90 was 25% and 12% less than the maximum load in beam S12-90. The deformation capacity was registered in the GR12-BD-90, GR12-BD-45 beams, corresponding to the maximum load at beam mid-span. In comparison with Δ_{ul-c} (Control) beam, the Δ_{ul} was 94% and 87% larger, respectively, as shown in Fig. 15. In comparison with Δ_{ul-s} (S12-90 beam), the Δ_{ul} was 4% and 8% less than the deformation capacity corresponding to the maximum load in the S12-90 beam, respectively. The deformation capacity corresponding to the crack load Δ_{cr} in these beams GR12-BD-90, GR12-BD-45 was 41% and 3% larger than the deformation capacity corresponding to the crack load in the (Control) beam Δ_{cr-c}. Finally, the specimens GR12-BD-90, GR12-BD-45 failed in shear at maximum load 152.9, 177.8 KN, respectively.

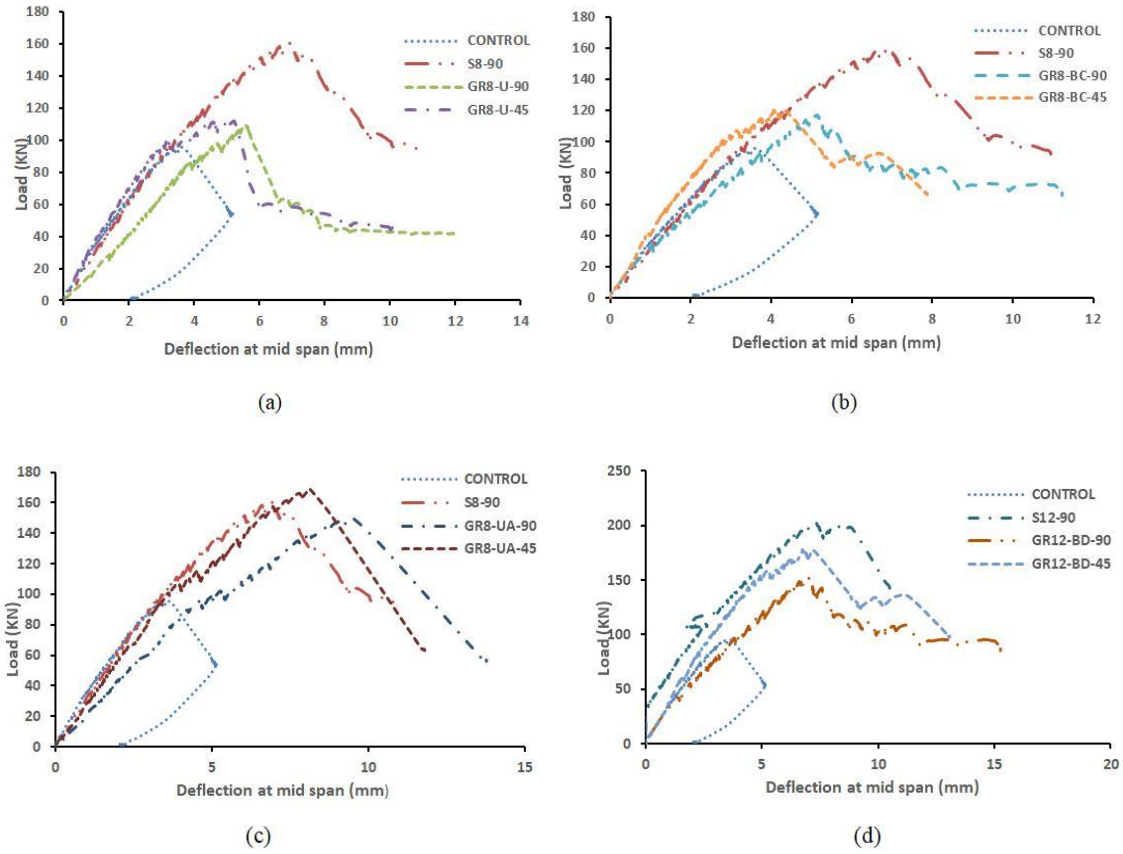

Fig. 8. Load - deflection relationship of series A

3.1.3 Series B

3.1.3.1 Specimens GS8-B-90 and GS8-UR-90

For these beams strengthened with GFRP by (EBR) technique with strips (Box – shape), strips (U – shape with top rod), Fig. 6 shown the crack pattern in these specimens. The relationship between the maximum load and the deflection at beam mid-span is depicted in Fig. 9. Table 3 includes the main results obtained in these specimens. Taking the maximum load of (Control) beam as a reference value, the GS8-B-90, GS8-UR-90 beams provided a 22% and 7% increase in maximum load, respectively as shown in Fig. 10. The GS8-UR-90 specimen recorded the least load capacity. The crack load of these specimens GS8-B-90, GS8-UR-90 was 2% and 1% larger than the crack load of the (Control) beam, respectively. When compared the maximum load in this specimens with beam strengthening with inner steel stirrups S8-90 was 27% and 36% less than the maximum load in beam S8-90. The deformation capacity was registered in the GS8-B-90, GS8-UR-90 beams, corresponding to the maximum load at beam mid-span. In comparison with $\Delta_{ul\text{-}c}$ (Control) beam, the Δ_{ul} was 59% and 19% larger, respectively as shown in Fig. 15. In comparison with $\Delta_{ul\text{-}s}$ (S8-90 beam), the Δ_{ul} was 17% and 39% less than the deformation capacity corresponding to the maximum load in the S8-90 beam, respectively. The deformation capacity corresponding to the crack load Δ_{cr} in these beams GS8-B-90, GS8-UR-90 was 24% and 15% larger than the deformation capacity corresponding to the crack load in the (Control) beam $\Delta_{cr\text{-}c}$. Finally, the specimens GS8-B-90, GS8-UR-90 failed in shear at maximum load 116.65, 102.4 kN, respectively. By comparing the previous samples with samples GS8-B-90 and GS8-UA-90 it was observed that the (NSM) technique has an effective effect in shear resistance of the (EBR) technique.

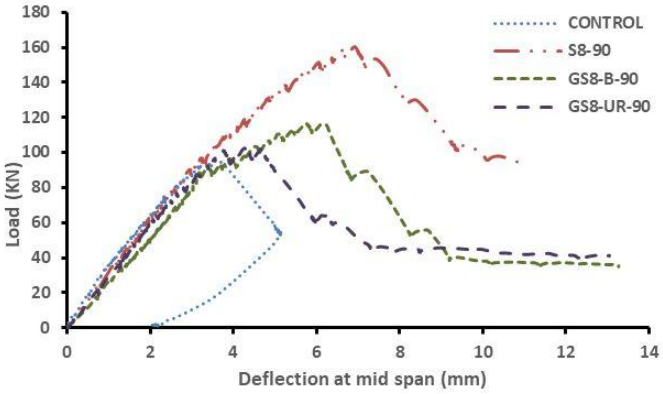

Fig. 9. Load - deflection at mid span relationship of series B

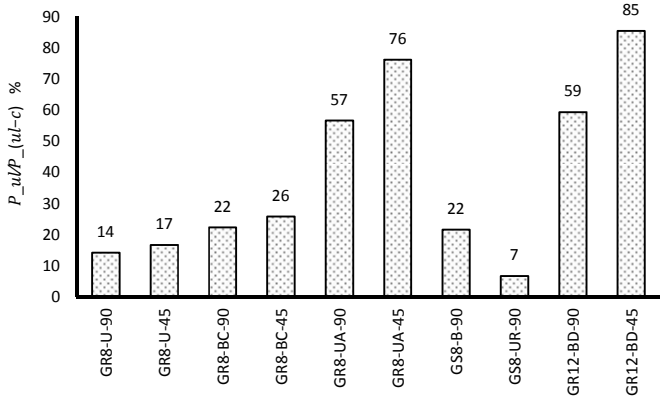

Fig. 10. Influence of the strengthening using GFRP bars, strips

3.2 Failure Modes

Figs. 6 and 7 showed the crack patterns and failure modes for all specimens. As was expected, all the tested specimens failed in shear, when the maximum load was reached. (Control) beam, without any reinforcement in shear, had failed by the formation of shear failure crack without the yielding of the longitudinal tensile reinforcement. A shear failure crack occurred in the specimens strengthened with steel stirrups. However, in specimens S8-90, S12-90 this shear failure crack occurred after the yielding of the longitudinal tensile reinforcement. In specimens strengthened with GFRP rods with NSM technique, GR8-U-90, GR8-U-45 in these specimens the failure occurred due to the separation of large parts of concrete cover, but larger in GR8-U-90. As shown in Fig. 7(a) – (b), respectively. In GR8-BC-90, GR8-BC-45 After the formation of the critical shear crack in this beams, debonding between GFRP rod and epoxy and separation for parts of concrete cover caused specimens to fail. As shown in Figs. 7(c) – (d), respectively. After the formation of the critical shear crack in beam GR8-UA-90, the failure was not due to pure debonding between the GFRP rod and epoxy or the epoxy and concrete surface. Based on post-failure inspections, it was due to the formations of the crack in the concrete cover leading to the separation of part of concrete cover from the beam. As shown in Fig. 7(e). The beam GR8-UA-45 failed due to GFRP rod rupture at the junction between the GFRP rod and the anchorage as shown in Fig. 7(f). After this rupture occurred, some parts of the concrete cover surrounding the GFRP rod were peeled away. In GR12-BD-90, GR12-BD-45 After the formation of the critical shear crack in these beams, the failure was due to debonding between the GFRP rod and epoxy, leading to the separation of a large part of concrete cover from the beam as shown in Fig. 7(g) – (h). After the formation of the critical shear crack in beam GS8-B-90, the failure was due to debonding between the GFRP strip and concrete surface, rupture the GFRP, leading to the separation of a large part of concrete cover from the beam Fig. 7(i). The beam GS8-UR-90 failed due to GFRP rupture at the bottom as shown in Fig. 7(j).

3.3 Discussion

3.3.1 Effect of the spacing between stirrups

Fig. 11 showed the effect of spacing between GFRP rods stirrups, as the spacing between the NSM GFRP rods in the orthogonal direction decreases, ultimate load capacity increases but at a low rate. As the spacing between the NSM GFRP rods in the orthogonal direction is decreased the interaction between the bond stresses around adjacent GFRP stirrups gets strengthened and hence the formation of failure pattern is accelerated. Thus, decreasing the spacing between the stirrups do not benefit the load capacity of the beams. In both cases, the reduced distance strengthens the interaction between the bond stresses around adjacent stirrups and hence accelerates the formation of failure patterns.

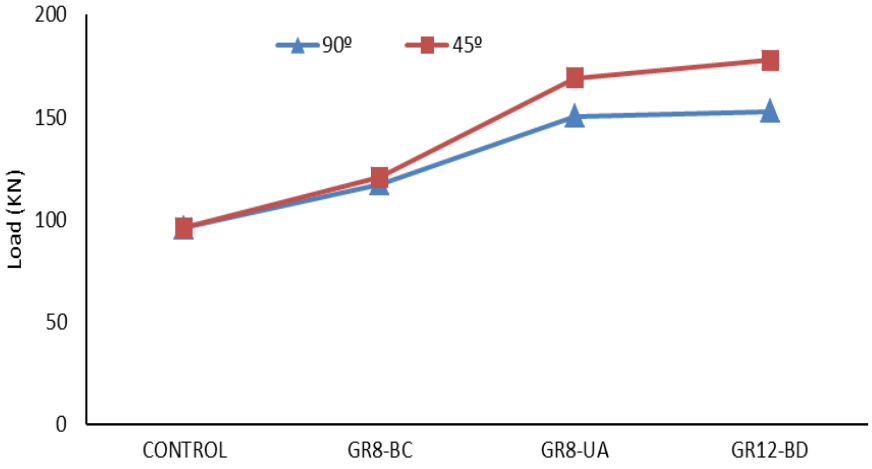

Fig. 11. The effect of spacing between GFRP rods stirrups

3.3.2 Effect of the alignment of the stirrups with NSM

Fig. 12 showed the effect of the alignment of GFRP rods stirrups. At the specimens strengthened with inclined GFRP rods, an increase in carrying load capacity was observed more than specimens strengthened with vertical GFRP rods. It is also observed that inclined rods were more effective than vertical rods. This is justified by the orientation of the shear failure cracks that had a tendency to be almost orthogonal to inclined laminates. Furthermore, for vertical rods, the total resisting bond length of the GFRP is lower than that of inclined rods.

3.3.3 Effect of the end anchorage

Figs. 13 and 15 showed the influence of adding the end anchorage at the GFRP rods stirrups on the carrying load capacity and cracking load capacity and deflection. It is clear that the specimens strengthened with rods GFRP with end anchorage showed much better results than the other specimens. the ultimate load capacity and cracking load in specimen (GR8-UA-90) was increased by 37%, 36% compared to specimen (GR8-U-90) with GFRP rods without end anchorage, The deflection corresponding to the ultimate and crack load in specimen (GR8-UA-90) with anchored GFRP was increased by 70%, 98% compared to specimen (GR8-U-90) without end anchorage. It was due to the increased in the debonding length between GFRP rods and the concrete surface. Clearly, the use of GFRP rods with end anchorage in GR8-UA-90 and GR8-UA-45 specimens led to an enhancement in both the ultimate strength and the corresponding deflection.

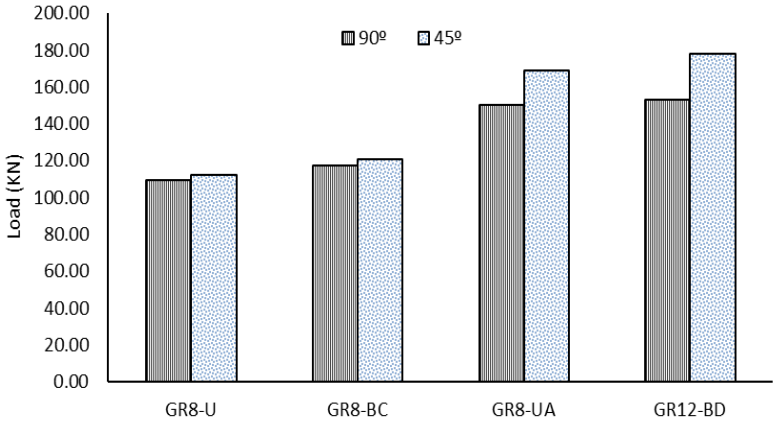

Fig. 12. The effect of the alignment of GFRP rods stirrups

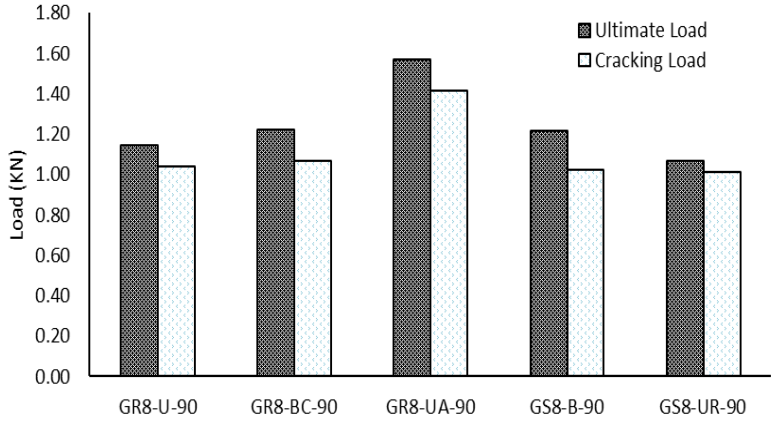

Fig. 13. The influence of add the end anchorage at the of GFRP rods stirrups

3.3.4 Effect of the strengthening technique

Fig. 14 showed the influence of the shear reinforcement technique on the ultimate load and crack load. The NSM technique was the most effective among the adopted GFRP shear strengthening configurations, and the EBR was the least effective configuration. The specimens strengthened with GFRP rods with the NSM technique showed significant improvement in the ultimate load and cracking load between (14% to 85%), and (1% to 45%) larger than the (Control) beam, respectively, while the increase was low in the ultimate load in specimens strengthened with the EBR technique 7% to 22%, but the cracking load showed no improvement.

3.3.5 Effect of the strengthening technique on the deformability indices

Fig. 15 showed the influence of the shear strengthening technique on deformation capacity. Clearly, the use of GFRP rods with end anchorage led to an enhancement in the ultimate deflection and crack deflection. The highest deformation capacity was registered in the specimens strengthened with GFRP rods with end anchorage GR8-UA-90, GR8-UA-45. At both the deflection corresponding ultimate load and crack load In comparison with (Control) specimen (unreinforced beam) is between 164%, 126% and 195%, 103% larger, respectively.

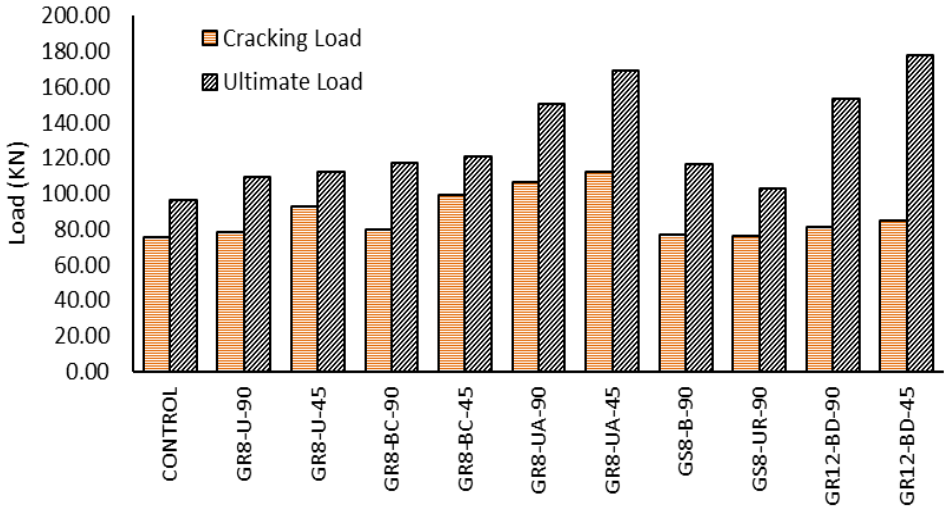

Fig. 14. The influence of the shear reinforcement technique on ultimate load and crack load

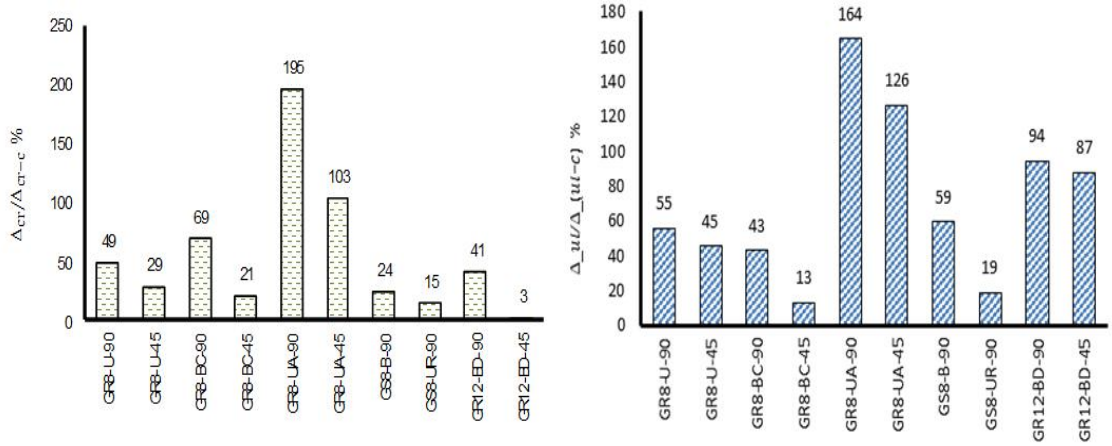

Fig. 15. The influence of the shear strengthening technique on deformation capacity

4. CONCLUSIONS

From the study conducted on the shear strengthening of reinforced concrete beams (RC) using near surface mounted (NSM) technique using GFRP in different types like rods, strips. In different alignments and spacing's and different end anchorage; from this study, the following conclusions can be made:

- GFRP rods, strips are found to be effective in the shear strengthening of reinforced concrete beams RC.
- The strengthened specimens showed improvement in all terms like deflection characteristics, first crack load, and ultimate load when compared to the control specimen.
- The use of near surface mounted (NSM) technique was more efficient than externally bonded reinforcement technique (EBR) in shear strengthening. When compared between the shear capacity of RC beams strengthened with NSM with those of RC beams externally bonded reinforcement with GFRP side sheets with the same amount of fiber Confirmed that the performance of the NSM better than EBR side strips.
- The ultimate shear of all the strengthened beams was more than that of the control beam.
- The samples strengthened with (NSM) technique by using GFRP rods U shape with anchorage, showed an improvement in the ultimate load compared to the samples strengthened with (NSM) technique by using GFRP rods U shape without a cap. But when compared with the control sample, the load was improved significantly. The increase in the shear capacity was between 57% and 76% for these specimens.
- The specimens strengthened with (NSM) technique by using GFRP rods U shape with strand, showed an improvement in the ultimate load compared to the control specimens, As a result of the reduction of the distance between the GFRP rods. The increase in the shear capacity was between 59% and 85% for these specimens.
- The test results have confirmed that the use of Anchorage at the end of rodsis effective for improving the shear capacity of reinforced concrete beams.

ACKNOWLEDGEMENTS

The authors wish to offer their sincere gratitude to the staff of reinforced concrete laboratory of the department of Civil Engineering, Benha University, Benha, for their support and collaboration during the course of this research.

COMPETING INTERESTS

Authors have declared that no competing interests exist.

REFERENCES

1. AL-Salloum, Yousef A, et al. Effect of harsh environmental conditions on the tensile properties of GFRP bars. Composites Part B: Engineering. 2013;45.1:835-844.
2. Mosallam, Ayman S. Banerjee, Swagata. Shear enhancement of reinforced concrete beams strengthened with FRP composite laminates. Composites Part B: Engineering, 2007;38.5-6:781-793.
3. Eslami A, Ronagh Hamid R. Experimental investigation of an appropriate anchorage system for flange-bonded carbon fiber–reinforced polymers in retrofitted RC beam–column joints. Journal of Composites for Construction. 2013;18.4:04013056.
4. Mostofinejad Davood, Mahmoudabadi Ehsan. Grooving as alternative method of surface preparation to postpone debonding of FRP laminates in concrete beams. Journal of Composites for Construction. 2010;14.6:804-811.
5. Moshiri, Niloufar, et al. Experimental and analytical study on CFRP strips-to-concrete bonded joints using EBROG method. Composites Part B: Engineering. 2019;158:437-447.
6. Dalalbashi A, Eslami A, Ronagh Hamid R. Plastic hinge relocation in RC joints as an alternative method of retrofitting using FRP. Composite Structures. 2012;94.8: 2433-2439.
7. Deng Jiangdong, et al. Interfacial mechanical behaviors of RC beams strengthened with FRP. Structural Engineering and Mechanics. 2016;58.3: 577-596.
8. Kocak Ali. Earthquake performance of FRP retrofitting of short columns around band-type windows. Structural Engineering and Mechanics. 2015;53.1:001-16.

9. Baji Hassan, Eslami A, Ronagh Hamid R. Development of a nonlinear FE modelling approach for FRP-strengthened RC beam-column connections. In: Structures. Elsevier. 2015;272-281.
10. Dalalbashi A, Eslami A, Ronagh Hamid R. Numerical investigation on the hysteretic behavior of RC joints retrofitted with different CFRP configurations. Journal of Composites for Construction. 2013;17.3: 371-382.
11. Dias Salvador JE, Barros Joaquim AO. Shear strengthening of RC beams with NSM CFRP laminates: Experimental research and analytical formulation. Composite Structures. 2013;99: 477-490.
12. Bianco Vincenzo, Monti Giorgio, Barros Joaquim AO. Design formula to evaluate the NSM FRP strips shear strength contribution to a RC beam. Composites Part B: Engineering. 2014;56:960-971.
13. Ramezanpour M, Morshed R, Eslami A. Experimental investigation on optimal shear strengthening of RC beams using NSM GFRP bars. Structural Engineering and Mechanics. 2018;67.1:45-52.
14. Rjoub AL, Yousef S, et al. Shear strengthening of RC beams using near-surface mounted carbon fibre-reinforced polymers. Australian Journal of Structural Engineering. 2019;20.1:54-62.
15. Khalifa Ahmed, Nanni Antonio. Rehabilitation of rectangular simply supported RC beams with shear deficiencies using CFRP composites. Construction and Building Materials. 2002;16.3:135-146.
16. Rizzo Andrea, Lorenzis DE, Laura. Behavior and capacity of RC beams strengthened in shear with NSM FRP reinforcement. Construction and Building Materials. 2009;23.4:1555-1567.
17. Lorenzis DEL, Teng JG. Near-surface mounted FRP reinforcement: An emerging technique for strengthening structures. Composites Part B: Engineering, 2007;38.2:119-143.
18. Jayaprakash J, et al. Shear capacity of precracked and non-precracked reinforced concrete shear beams with externally bonded bi-directional CFRP strips. Construction and Building Materials. 2008;22.6:1148-1165.
19. Hassan Tarek, Rizkalla Sami. Flexural strengthening of prestressed bridge slabs with FRP systems. PCI Journal. 2002;47.1: 76-93.
20. Kachlakev D, Mccurry DD. Behavior of full-scale reinforced concrete beams retrofitted for shear and flexural with FRP laminates. Composites Part B: Engineering, 2000;31.6-7:445-452.
21. Sundarraja MC, Rajamohan S. Strengthening of RC beams in shear using GFRP inclined strips–An experimental study. Construction and Building Materials. 2009;23.2:856-864.
22. Täljsten Björn, Elfgren Lennart. Strengthening concrete beams for shear using CFRP-materials: Evaluation of different application methods. Composites Part B: Engineering. 2000;31.2:87-96.
23. Hassan Tarek, Rizkalla Sami. Investigation of bond in concrete structures strengthened with near surface mounted carbon fiber reinforced polymer strips. Journal of Composites for Construction. 2003;7.3:248-257.
24. Zhang Zhichao HSU, Cheng-Tzu Thomas. Shear strengthening of reinforced concrete beams using carbon-fiber-reinforced polymer laminates. Journal of Composites for Construction. 2005;9.2:158-169.

Peer-review history:
The peer review history for this paper can be accessed here:
http://www.sdiarticle3.com/review-history/49619